

## Sintering of Nanocrystalline Zinc Oxide via Conventional Sintering, Two Step Sintering and Hot Pressing

Mehdi Mazaheri<sup>1, 2\*</sup>

<sup>1</sup>Materials and Energy Research Center, Tehran, Iran

<sup>2</sup>Institute of Physics of Complex Matter, Swiss Federal Institute of Technology Lausanne (EPFL), 1015 Lausanne, Switzerland

### Abstract

Two-step sintering and hot pressing methods were applied on nanocrystalline ZnO to control the accelerated grain growth occurring during the final-stage of sintering. The sintering conditions (temperature and total time) and results (density and grain size) of two-step sintering (TSS), conventional sintering (CS) and hot pressing (HP) methods were compared. The grain size of the high density (>98%) ZnO compact produced by the two-step sintering was smaller than 1  $\mu\text{m}$ ; while the grain size of those formed by the conventional sintering method was  $\sim 4 \mu\text{m}$ . The HP technique versus CS was shown to be a superior method to obtain higher final density (99%), lower sintering temperature, shorter total sintering time and rather fine grain size. The maximum density achieved via HP, TSS and CS methods were 99%, 98.3% and 97%, respectively. The final grain size of samples obtained by HP was larger than that of TSS method. However, the ultra-prolonged sintering total time and the lower final density (88 ks and 98.3%) are the drawbacks of TSS in comparison with the faster HP (17 ks and 99%) method.

### Introduction

ZnO is an attractive ceramic material usable in electrical, optical and medical applications [1-3]. Due to photoluminescence properties, ZnO is used in green displaying devices. Because of the high volume of grain boundaries in the as-produced nanocrystalline ZnO ceramics by SPS, these materials produce both strong-green and weak-ultraviolet emissions [2-7]. These materials are also used in the production of varistors, gas sensors, ultrasonic transducers and surface-acoustic-wave (SAW) devices due to their high piezoelectricity. Identical to the optical properties, the electrical ones strongly depend on the density and microstructure uniformity. The properties of ZnO varistors have, for instance, been reported to be highly influenced by proportion of grain boundaries [6-9]. Kiselev *et al.* [8] have shown that if the value of the grain boundary depletion-length is fixed, increasing grain size can decline the conduction nonlinearity. Duran *et al.* [7] have reported that a breakdown voltage for the varistors increases by decreasing the grain size.

There have been three main approaches, usually applied to avoid the accelerated grain growth associated with densification and, therefore, provide fine microstructures. The first one is the addition of second phase particles (dopants) to modify diffusion processes, prevent the grain boundary migration and, hence,

suppress the grain growth. Nevertheless, the second phase can be destructive to densification and physical behavior. Han *et al.* [10] have, for instance, shown that, while the addition of Al significantly inhibits the grain growth of ZnO and increases the grain growth kinetic exponent from 3 to 6 for pure and Al-Doped ZnO, respectively, the ZnO system is a notable decline in the densification rate. Sedky *et al.* [11] have studied the sintering behavior of Fe-doped ZnO samples. They have reported that in spite of the grain growth suppression caused by the Fe content, the abovementioned approach diminishes final density of the sintered specimens. On the other hand, their investigation exposed the detrimental effect of Fe dopants on the electrical conductivity of pure ZnO samples.

The second approach is a new technique called the two-step sintering (TSS). This method offers a promising approach for fabrication of bulk nanograin ceramics, thereby, exploiting the difference in kinetics between grain boundary diffusion and grain boundary migration [12, 13]. TSS is carried out by the high temperature firing, followed by rapid cooling and low temperature holding of the samples. Using the two-step sintering method, the authors managed to manufacture submicrometer grained ZnO bodies for the first time in their previous work [14].

The third is the use of particular consolidation techniques, such as hot pressing or spark plasma sintering. The application of external pressure increases the driving force for densification. Hot pressing provides one of the most reliable techniques to adjust the relative rates of densification [15, 16].

According to the best knowledge of the authors, few reports are available in the literature talking over the densification and grain growth, during hot pressing of nanocrystalline ZnO samples. Hynes *et al.* [17] hot pressed nanophase ZnO compacts (at 60 MPa and 550°C for 30 min) to obtain bodies with the relative density of 95% TD. But, they do not have any clear report on densification and grain growth during the hot pressing method. In the present work, the densification and microstructural evolution of samples during hot pressing were investigated. The sintering conditions (such as total time and temperature of sintering) and results (final density and grain size) of HP, CS and TSS methods were compared.

## Experimental procedure

### Raw material

Pure (>99.7%) ZnO nanopowder was obtained from Inframmat Advanced Materials Farmington, CT. Morphological studies and particle size determinations were performed by transmission electron microscopy (TEM, CM200 FEG, Philips, Netherlands). According to the supplier, the specific surface area of the powder determined by Brunauer-Emmett-Teller (BET) method was  $35 \text{ g}\cdot\text{cm}^{-3}$ .

### Compaction

The powder was uniaxially cold-pressed at 200 MPa into pellets with diameter of 10.2 mm and thickness of 3 mm. Based on the ZnO theoretical density (TD) of  $5.606 \text{ g}\cdot\text{cm}^{-3}$ , the average green density of the nanocrystalline ZnO powder compacts was determined to be  $\sim 0.61 \text{ TD}$  after pressing.

### Conventional and two-step sintering

Sintering of the green bodies was carried out by conventional (CS) and two-step sintering (TSS) methods. CS was carried out at 600 to 1200°C in air with 50°C temperature intervals and a heating ramp of  $0.05^\circ\text{C}\cdot\text{s}^{-1}$ . The specimens were held at the highest temperature for 60 s in order to obtain a uniform temperature throughout the sample. For the first step of TSS, the samples were heated under the same conditions as conventional sintering. The cooling rate of TSS between  $T_1$  to  $T_2$  was  $1^\circ\text{C}\cdot\text{s}^{-1}$ . The samples were held at  $T_2$  up to 72 ks so as to reach a higher density.

### Hot pressing

The powder was hot pressed at the pressure of 50 MPa using cylindrical graphite dies coated with boron nitride with an inner diameter of 10 mm. The sintering temperature varied from 400 to 850°C with interval of 50°C. The heating rate was adjusted at  $0.05^\circ\text{C}\cdot\text{s}^{-1}$ . After heating to maximum temperature, the specimens were held at this temperature for 1 min, so as to yield a homogenous temperature in the whole body of the samples.

### Characterization

The density of the sintered sample was measured by the water displacement (Archimedes) method. For microstructural characterization, sintered pellets were fractured and then studied using scanning electron microscopy (SEM, Philips XL30, Netherlands). An image analyzer calculated the mean grain size of the samples.

## Results and Discussion

Fig. 1 represents TEM micrographs of the nanocrystalline ZnO powder. It can be observed that particles are mainly of a round shape and the particle size ranges from 20 to 40 nm. According to the information given by the supplier, the specific surface area of the powder determined by Brunauer-Emmett-Teller (BET) method was  $35 \text{ m}^2\cdot\text{g}^{-1}$ . The particle size, determined by the TEM observation, is in good

agreement with the average particle size, calculated from the BET result ( $\sim 31 \text{ nm}$ ).

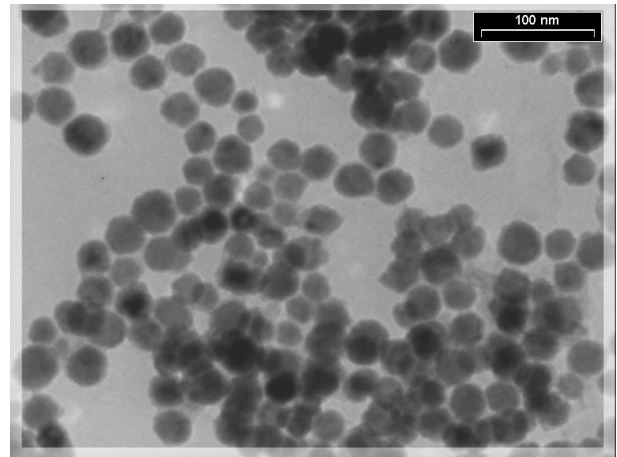


Fig. 1 Transmission electron microscopy (TEM) micrograph of nanocrystalline ZnO.

Fig. 2 shows the variation of density and grain size of hot pressed nanocrystalline ZnO versus sintering temperatures. As shown in this figure, the sintering plot exhibits a sigmoidal shape. The densification starts at around 450°C and the densification rate increases dramatically with the temperature rise up to 600°C. It can be seen that a 200°C increase (from 500°C to 700°C) in temperature results in the fractional density evolution from  $\sim 0.65$  to  $\sim 0.95$ . The specimens with the relatively full density of 99% TD are produced by hot pressing at 850°C. As it can be seen, the grain size of ZnO samples increases with the temperature and the rate of grain growth shows a significant improvement at temperatures higher than 650°C. The dense ZnO samples, sintered at 850°C, have microstructures with the mean grain size of about  $1.4 \mu\text{m}$ . From the above experimental results and analysis, it can be found that despite improving the sample density, an increase in the sintering temperature increases the grain size. Employing the pressure through the sintering procedure is not only helpful to remove the porosities from the powder compacts but also provides an additional driving force for densification and, hence, yields full dense samples (99% of TD).

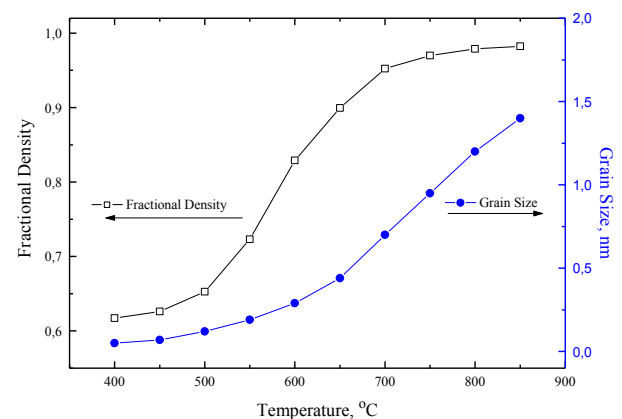


Fig. 2. Fractional density and grain size of hot pressed nanocrystalline ZnO under 50 MPa versus temperature.

Final densities achieved by hot pressing and conventional sintering are displayed in Fig. 3 as a function of temperature. As shown in this figure, CS, generally, results in the significantly lower densities than HP at equivalent temperatures, and the densification starts  $\sim 200^\circ\text{C}$  earlier when the pressure is applied during the HP.

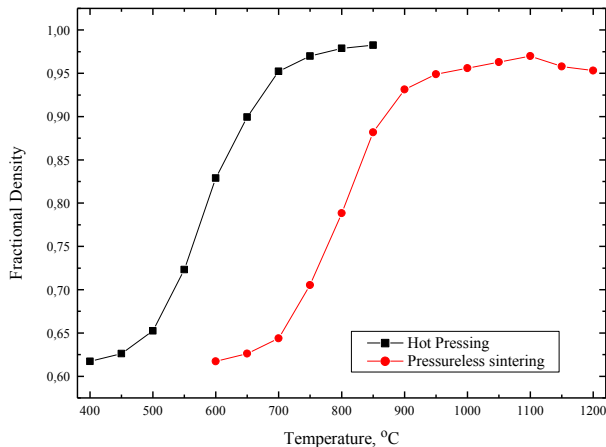


Fig. 3 Fractional density of hot pressed and conventionally sintered nanocrystalline ZnO compacts versus temperature.

In order to have an accurate comparison between TSS, HP and CS methods, the results concerning the sintering path (grain size versus fractional density) are presented in Fig. 4.

The results (Fig. 4) indicate that, no matter both methods of CS and HP show the parabolic growth in the sintering final stage (fractional density  $> 90\%$ ), the grain growth tends to follow a moderate trend during the HP in comparison with CS. In contrast, the results of TSS method demonstrate no trace of the triggered growth, even in the final stage of sintering.

The fact is that the grain growth is not directly contributed by the applied pressure. The effect of an external pressure, therefore, becomes more obvious in the system when the grain growth rate relative to the densification rate is high (for example, in the sintering final stage of CS (Fig. 4)). Since the application of an external pressure in the system increases the densification rate, it leads to a reduction of sintering temperature (Fig. 3) and consequently, to the further grain growth suppression (Fig. 4). As it was presented in many previous publications [12-14], the TSS method is naturally a favorable method to control the grain growth during densification in the final stage of sintering. The lower sintering temperature ( $T_2$ ) in the TSS second step is the parameter to account for decent grain growth suppression provided by this method. The immobile triple point junctions, at this low temperature ( $T_2$ ), can suppress the grain boundaries as the major motivator of the grain growth, while the grain boundary diffusion is still active to obtain near full dense samples (detail of TSS condition for nanocrystalline ZnO is available in [14]).

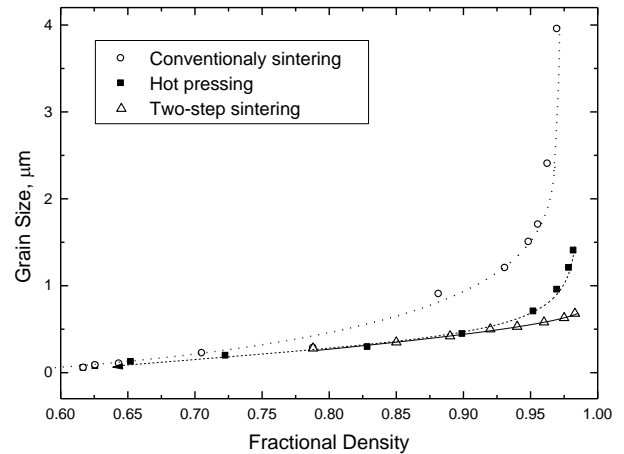


Fig. 4 Sintering path (grain size/fractional density) for sintered nanocrystalline ZnO compacts by three different method.

Fig. 5 shows the fractional density of the samples sintered via three different methods versus the total time of sintering. Although the two-step sintered specimens have smaller grains than the hot pressed bodies, the ultra-prolonged sintering time of TSS method as well as the lower density of the specimens have set severe restrictions on the technological application of this method (see Fig. 5). The HP is, therefore, an efficient method to remove the problems that many other sintering techniques are involved in. This high efficiency stems from two major aspects, i.e. first, the high pressure that accelerates the densification process and second, the lower sintering temperature (Fig. 3) of the powder together with the shorter sintering time (Fig. 5) that result in a sharp decrease in the grain size of the specimens.

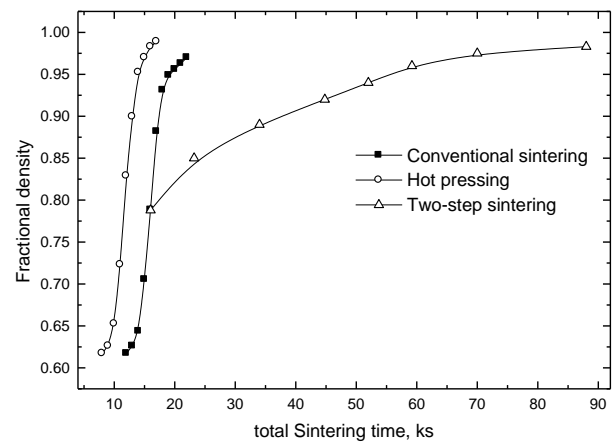


Fig. 5 Fractional density of samples sintered using three different methods versus total time of sintering.

On the other hand, Fig. 4 shows the capability of HP to produce the specimens with higher density (99%) than CS (97%) and TSS (98.3%) methods. In the case of ZnO nanoparticles, two significant problems are likely to happen at higher temperatures ( $> 1000^\circ\text{C}$ ) that retard the densification around 97% TD. The first problem is aroused by the insoluble gas entrapped in the pores [17]. Mazaheri *et al.* [14], have, For instance, shown that in higher temperatures than  $1100^\circ\text{C}$  (in the case of

nanocrystalline ZnO), an increase in the gas pressure entrapped in the pores may prohibit the mass transport caused by the diffusion mechanisms. The second problem is the material loss (including zinc and oxygen) from the surface of the powder to the furnace wall that results in a decrease in the final density at higher temperatures. There are also some investigations in the literature that prove the dramatic weight loss above 1100°C, using thermogravimetric analysis (TGA) [14, 17]. Thus, the density increase from 1100°C to 1200°C not only results in the exaggerated grain growth but also reduces the final density (see Fig. 3). Meanwhile, as the HP declines the sintering temperature, the mentioned problems are removed as a result of applying this method. The lower sintering temperature in the HP also, results in a lower pressure of insoluble gas. On the other hand, the applied pressure during the HP method can act as an opponent factor against gas pressure. Thus, the porosity can collapse easier than in the CS method. Besides, in the case of CS, when the pressure of entrapped gas becomes equal to the capillary pressure of the pore, the pore stops shrinkage and the maximum attainable sintered density is reached. The application of an external pressure after the pore isolation can, hence, increase the sintered density up to a higher value than that by the CS method. Additionally, according to the TGA results [14], at the hot pressing temperatures of < 850°C, the material loss from the surface of the particle was not observed.

## Conclusions

1. A relatively full density of 99% TD with the mean grain size of about 1.4  $\mu\text{m}$  was obtained for the samples, hot pressed at 850°C.
2. The comparative studies showed that the sintering efficiency of HP is higher than other methods and it managed to provide the maximum density for the HP specimens.
3. The final grain size of the hot pressed specimens was found to be larger than that of TSS method. However, the ultra-prolonged sintering total time concerning two-step sintering and the lower density of the specimens restrict the practical application of this method.

## References

1. L. Gao, Q. Li, W. Luan, *J. Am. Ceram. Soc.* **85** (2002) 1016-1018.
2. J. Wang, L. Gao, *J. Am. Ceram. Soc.* **88** (2005) 1637-1639.
3. B. A. Cottom, M. J. Mayo, *Scripta Mater.* **34** (1996) 809-814.
4. C.M. Mo, Y.H. Li, Y.S. Liu, Y. Zhang, L.D. Zhang, *J. Appl. Phys.* **83** (1998) 4389-4391.
5. K.F. Cai, X.R. He, L.C. Zhang, *Mater. Lett.* **62** (2008) 1223-1225.
6. D.R. Clarke, *J. Am. Ceram. Soc.* **82** (1999) 485-502.
7. P. Duran, J. Tartaj, C. Moure, *J. Am. Ceram. Soc.* **86** (2003) 1326-1329.
8. A.N. Kiselev, F. Sarrazit, E.A. Stepantsov, E. Olsson, T. Claeson, V.I. Bondarenko, R.C. Pond, N.A. Kiselev, *Philos. Mag. A* **76** (1997) 633-655.
9. T.K. Roy, D. Bhowmick, D. Sanyal, A. Chakrabarti, *Ceram. Int.* **34** (2008) 81-87.
10. J. Han, P.Q. Mantas, A.M.R. Senos, *J. Mater. Res.* **16** (2001) 459-468.
11. A. Sedky, M. Abu-Abdeen, A.A. Almulhem, *Physica B* **388** (2007) 266-273.
12. I.W. Chen, X.H. Wang, *Nature* **404** (2000) 168-171.
13. M. Mazaheri, M. Valefi, Z. Razavi Hesabi, S.K. Sadrnezhad, *Ceram. Int.* **35** (2009) 13-20.
14. M. Mazaheri, A.M. Zahedi, S.K. Sadrnezhad, *J. Am. Ceram. Soc.* **91** (2008) 56-63.
15. A. Weibel, R. Bouchet, R. Denoyel, P. Knauth, *J. Eur. Ceram. Soc.* **27** (2007) 2641-2646.
16. P. Dahl, I. Kaus, Z. Zhao, M. Johnsson, M. Nygren, K. Wiik, T. Grande, M.A. Einarsrud, *Ceram. Int.* **33** (2007) 1603-1610.
17. A.P. Hynes, R.H. Doremus, R.W. Siegel, *J. Am. Ceram. Soc.* **85** (2002) 1979-1987.

\*Corresponding author:  
 Mehdi Mazaheri  
[mehdi.mazaheri@epfl.ch](mailto:mehdi.mazaheri@epfl.ch)  
[mmazaheri@gmail.com](mailto:mmazaheri@gmail.com)  
 tel: +41 783 088880